Article:
Darby, J.F., Gilio, A.K., Piniello, B. et al. (2020) Substrate engagement and catalytic mechanisms of N-acetylglucosaminyltransferase V. ACS Catalysis, 10 (15). pp. 8590-8596. ISSN: 2155-5435

https://doi.org/10.1021/acscatal.0c02222

ACS Catalysis

pubs.acs.org/acscatalysis Letter

Substrate Engagement and Catalytic Mechanisms of N-Acetylglucosaminyltransferase V

John F. Darby,◆ Amelia K. Gilio,◆ Beatriz Piniello,◆ Christian Roth, Elena Blagova, Roderick E. Hubbard, Carme Rovira,* Gideon J. Davies,* and Liang Wu*

Cite This: *ACS Catal.* 2020, 10, 8590–8596 Read Online

ACCESS | Metrics & More | Article Recommendations | Supporting Information

ABSTRACT: α-Mannoside β-1,6-*N*-acetylglucosaminyltransferase V (MGAT5) is a mammalian glycosyltransferase involved in complex N-glycan formation, which strongly drives cancer when overexpressed. Despite intense interest, the catalytic mechanism of MGAT5 is not known in detail, precluding therapeutic exploitation. We solved structures of MGAT5 complexed to glycosyl donor and acceptor ligands, revealing an unforeseen role for donor-induced loop rearrangements in controlling acceptor substrate engagement. QM/MM metadynamics simulations of MGAT5 catalysis highlight the key assisting role of Glu297 and reveal considerable conformational distortions imposed upon the glycosyl donor during transfer. Detailed mechanistic characterization of MGAT5 will aid inhibitor development to correct cancer-associated N-glycosylation.

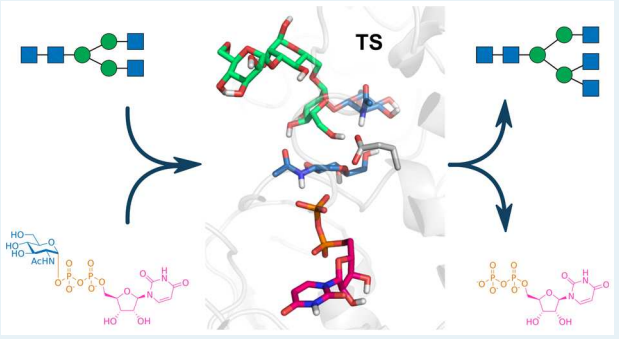

KEYWORDS: *enzymes, N-glycosylation, carbohydrates, glycosyltransferases, quantum mechanics/molecular mechanics*

Protein N-glycosylation—the attachment of a glycan to the nitrogen of an Asn side chain—is one of the most prevalent eukaryotic post-translational modifications,[1] estimated to decorate over half of all proteins.[2] N-Glycosylation of proteins serves diverse functions, including regulating protein folding[3] and stability.[4] Cell surface N-glycans modulate the properties of their underlying proteins and also engage directly with the extracellular matrix.[5] The formation and maturation of N-glycans is nontemplated, leading to the production of diverse protein glycoforms that reflect the function and physiological state of the cell.[6] Accordingly, changes to cellular N-glycosylation patterns are major features of malignant transformation, which can drive further oncogenic behavior in transformed cells.[7]

α-Mannoside β-1,6-N-acetylglucosaminyltransferase V (MGAT5, also GnT-V) is a mammalian medial-Golgi inverting glycosyltransferase, which transfers N-acetylglucosamine (GlcNAc) from a UDP-GlcNAc glycosyl donor on to the core α-1,6 mannose (Man) of an N-glycan acceptor (Figure 1). The resulting branched GlcNAc-β-1,6-Man linkage is a precursor for the formation of complex tri- and tetra-antennary N-glycans, which are elaborated in the trans-Golgi by the addition of Gal-β-1,4-GlcNAc (LacNAc) disaccharides and sialic acids.[8]

MGAT5 overactivity drives cancer aggression via increased LacNAc prevalence. LacNAcs on N-glycosylated membrane proteins bind galectins, forming cell-surface "lattices" that protect against endocytic turnover.[9] Pro-oncogenic growth factor receptors, which are typically heavily N-glycosylated, thus show reduced turnover and potentiated signaling upon MGAT5 induction.[10,11] Galectin binding can also activate angiogenic receptors, providing a noncanonical route toward tumor neovascularization.[12] Notably, the β-1,6 linked products of MGAT5 activity are preferentially elaborated by poly-LacNAc repeats (Figure 1),[13] which bind galectins with higher avidity and affinity.

Reducing MGAT5 activity inhibits tumor growth. Viral oncogene-induced tumor formation is severely suppressed in *Mgat5* negative mice.[14] Similarly, *Mgat5* knockdown in murine mammary adenocarcinoma cells reduces their tumorigenicity *in vivo*.[15] To date, very few effective small-molecule inhibitors of MGAT5 have been developed,[16−18] owing to a lack of understanding of MGAT5 enzyme−substrate interactions and catalytic mechanisms. In seminal work, Nagae et al. recently reported the crystal structure of an inactive MGAT5 mutant complexed to an acceptor glycan analogue, revealing details of the enzyme fold and its acceptor binding interactions.[19] However, the molecular basis for MGAT5 engagement with its donor substrate UDP-GlcNAc remains unknown, fundamentally limiting our understanding of the interactions that lead

Received: May 19, 2020
Revised: July 16, 2020
Published: July 16, 2020

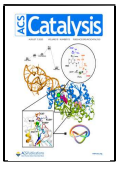

https://dx.doi.org/10.1021/acscatal.0c02222
ACS Catal. 2020, 10, 8590−8596

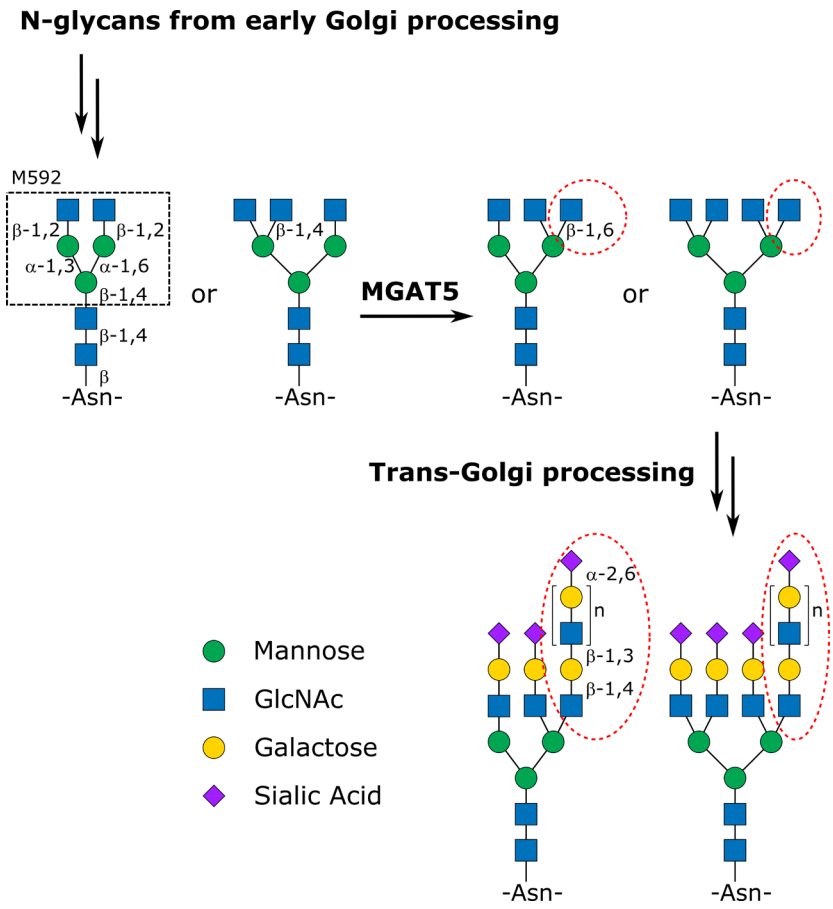

Figure 1. N-Glycan processing reaction catalyzed by MGAT5. β-1,6 linked products of MGAT5 activity are highlighted in red. The M592 pentasaccharide structure is highlighted in black.

Table 1. Kinetic Parameters for the Full Lys329−Ile345 Loop and Lys329−Ile345 Truncated MGAT5 Catalyzed Reactions[a]

	donor (UDP-GlcNAc)		acceptor (M592)	
	K_M/mM	k_{cat}/s^{-1}	K_M/mM	k_{cat}/s^{-1}
full Lys329−Ile345 loop	1.08 ± 0.21	0.06 ± 0.004	1.81 ± 0.07	0.35 ± 0.01
Lys329−Ile345 truncated	0.84 ± 0.30	0.16 ± 0.02	4.18 ± 1.19	1.08 ± 0.19

[a]Error ranges represent standard errors of the means. $N = 2$.

to glycosyl transfer. Here, we report novel structures of MGAT5 in complex with glycosyl donor and acceptor ligands, and use these structures to uncover the enzyme mechanism by means of quantum mechanics/molecular mechanics (QM/MM) simulations, thereby building a molecular overview of the MGAT5 catalytic cycle.

MGAT5 is a type-II-transmembrane enzyme, consisting of a cytoplasmic N-terminal domain, single pass transmembrane helix, linker sequence, and globular catalytic domain. Based on biochemical studies of rat *Mgat5*,[20] we designed a truncated human MGAT5 expression construct spanning Ser214−Ile741, omitting the transmembrane helix and the noncatalytic N-terminal domains of the enzyme. A second construct additionally incorporating a Lys329−Ile345−>$(Gly)_4$ loop truncation was also designed, following observations that the Lys329−Ile345 loop is dispensable for MGAT5 activity.[19] Both MGAT5 constructs expressed well in lepidopteran cells, and both showed robust *in vitro* activity in assays using the synthetic biantennary pentasaccharide M592 as a glycosyl acceptor. Kinetic parameters for transfer were broadly similar between the two constructs, although the Lys329−Ile345 truncated construct showed k_{cat} values consistently ∼3× higher than the full Lys329−Ile345 loop construct, and the full Lys329−Ile345 loop construct showed a ∼2.3× more potent K_M for M592 (Table 1; Figure S1). Compared with previous reports,[10,19,20] we also noted a higher acceptor substrate K_M in our assays, probably because of the minimal structure of M592 compared to previously used acceptors.

Our MGAT5 constructs crystallized readily in the $P2_12_12_1$ (full Lys329−Ile345 loop) and $P1$ (Lys329−Ile345 truncated) space groups (Table S1; Figure S2a), with similar folds to each other and to previously reported structures (Figure S3). Both crystal forms contained 2 MGAT5 molecules in the asymmetric unit (ASU), albeit with differing relative orientations of the protein monomers, suggesting no functional oligomer in solution (Figure S2b). $P2_12_12_1$ crystals typically diffracted poorly (below 3.5 Å resolution), although one highly anisotropic data set processed to 2.20 Å using STARANISO (Figure S4).[21] In contrast, $P1$ crystals consistently diffracted to better than 2 Å resolution, and were also highly amenable to ligand derivatization. Soaking $P1$ crystals with M592 (acceptor substrate) or UDP (donor product) produced binary cocrystal complexes

https://dx.doi.org/10.1021/acscatal.0c02222
ACS Catal. 2020, 10, 8590−8596

with clearly interpretable electron density in the MGAT5 acceptor or donor subsites, respectively.

Protein interactions in our MGAT5-M592 binary complex were mainly directed toward the M592 α-1,6-branch GlcNAc, which anchors the glycan within the acceptor subsite. This 1,6-branch GlcNAc is added to nascent N-glycans by MGAT2/GnT-II, highlighting the dependence of MGAT5 upon earlier enzymes in the N-glycan processing pathway. We also observed direct H-bonds to M592 from Asp378, Ser379, and Lys554, a CH-π interaction from Trp401, and H-bonds from symmetry related Glu258 and Glu263 side chains (Figure 2). Inverting glycosyltransferases such as MGAT5 are expected to operate via a one-step S_N2 type mechanism, with nucleophilic attack by the acceptor onto the glycosyl donor assisted by a catalytic base residue from the enzyme.[22] Surprisingly, we observed no interaction between the acceptor nucleophile (the M592 α-1,6 mannose O6) and the putative MGAT5 catalytic base Glu297, which instead coordinated to the nearby Ser379 side chain and GlcNAc acetamide. Thus, our MGAT5-M592 complex and the pseudoacceptor complex previously reported by Nagae[19] (Figure S5) likely correspond to catalytically inert MGAT5 configurations.

No MGAT5 complexes with donor subsite ligands have been reported to date, and the effects of donor binding on MGAT5 activity are poorly understood. Our MGAT5-UDP binary complex revealed that UDP binding induces extensive reordering of the MGAT5 Lys279−Gly293 loop (Figure 3), which is otherwise highly mobile in structures lacking donor subsite occupation (our unliganded and M592 structures and those from Nagae[19]). Lys279−Gly293 loop ordering was primarily driven by H-bonding between the UDP pyrophosphate and the backbone amides of Leu295 and Gly296, with H-bonds also observed from UDP to Lys454, Tyr452, Glu526, Leu497, and Ala523, as well as a molecule of ethylene glycol

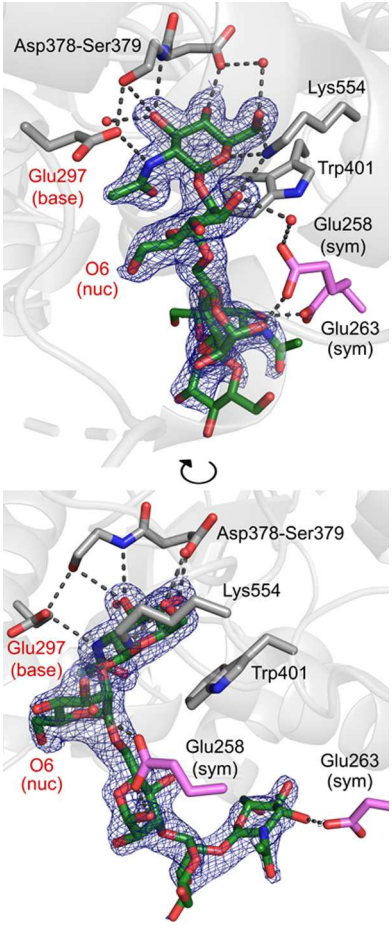

Figure 2. MGAT5 (gray) binary complex with the M592 pentasaccharide (green). Symmetry related residues in pink. No interaction is observed between the MGAT5 catalytic base (Glu297) and the acceptor nucleophilic atom (O6). Electron density is REFMAC σ_A-weighted 2mFo−DFc, contoured to 1σ (0.29 $e^{-}\cdot Å^{-3}$).

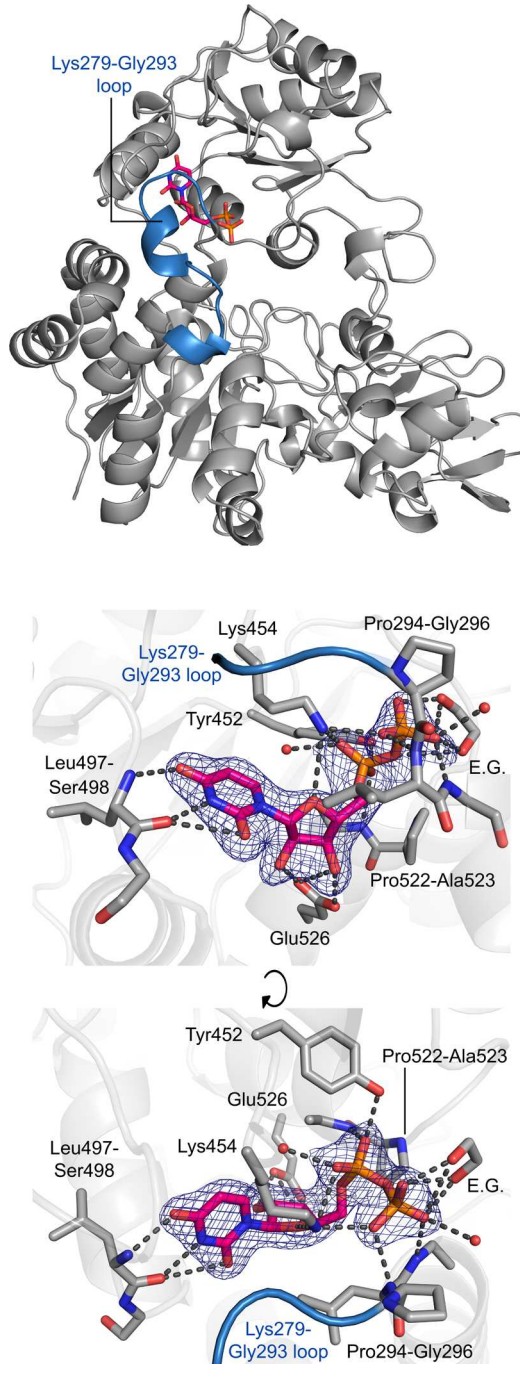

Figure 3. MGAT5 (gray) binary complex with UDP (pink). The Lys279−Gly293 loop (blue) is ordered upon occupation of the donor subsite. Electron density is REFMAC σ_A-weighted 2mFo−DFc, contoured to 1σ (0.20 $e^{-}\cdot Å^{-3}$). E.G.: ethylene glycol.

https://dx.doi.org/10.1021/acscatal.0c02222
ACS Catal. 2020, 10, 8590−8596

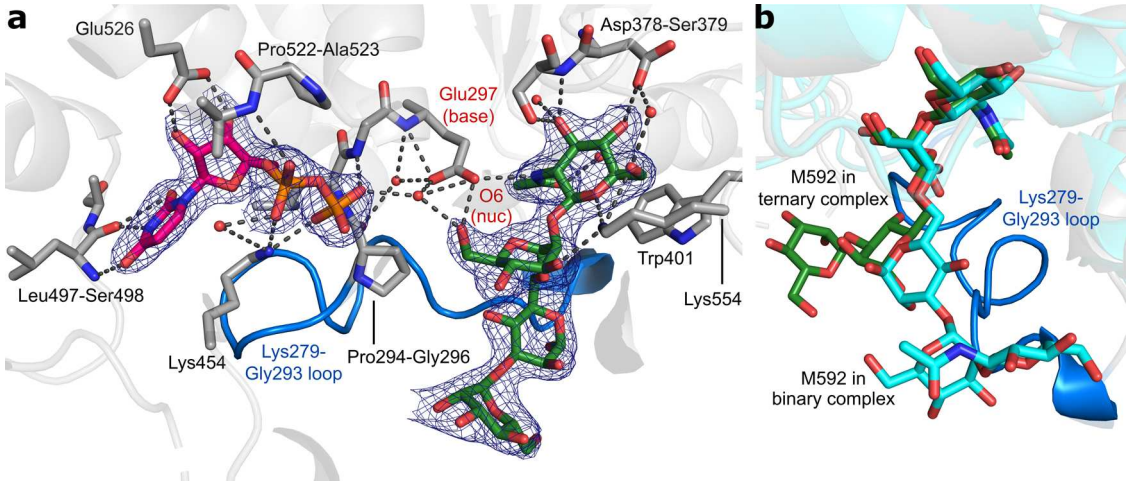

Figure 4. MGAT5 (gray) ternary complex with UDP (pink) and M592 (green). (a) Occupation of both donor and acceptor subsites enables the MGAT5 catalytic base (Glu297) to coordinate the acceptor nucleophile atom (O6) of M592. (b) Displacement of M592 by the ordered Lys279–Gly293 loop in the UDP+M592 ternary complex, compared with its binary complex (cyan); see also Figure S7a. Electron density is REFMAC σ_A-weighted 2mFo–DFc, contoured to 1σ (0.20 $e^{-}\cdot Å^{-3}$).

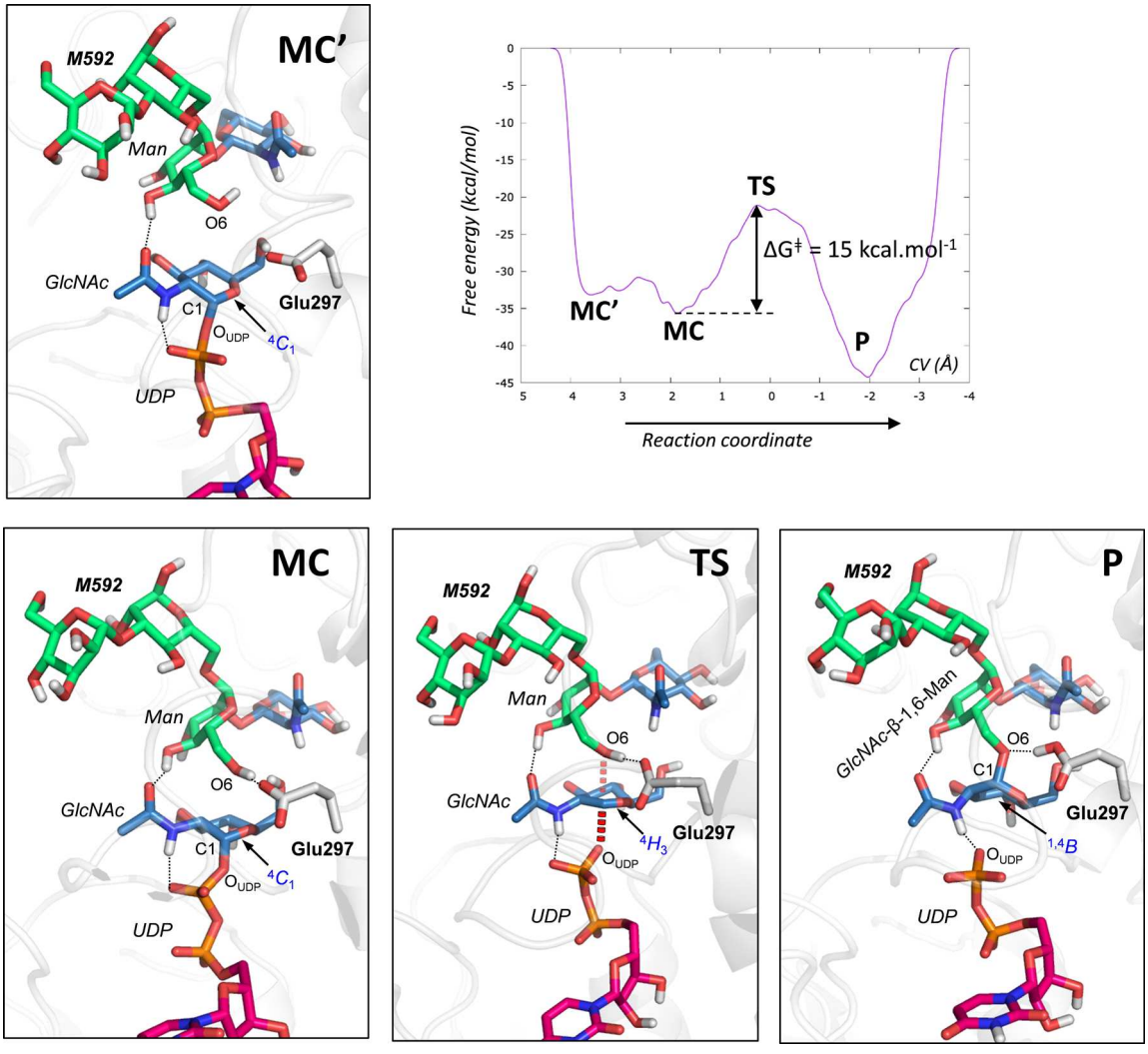

Figure 5. Atomic rearrangement along the glycosyl transfer reaction coordinate (**MC′**: pre-Michaelis complex; **MC**: Michaelis complex; **TS**: transition state; **P**: product complex). The transferred GlcNAc undergoes electrophilic migration from UDP-GlcNAc to the acceptor α-mannose O6, with clear oxocarbenium-like character at **TS**. Red dashes: bonds broken/formed. Black dashes: relevant H-bonds.

https://dx.doi.org/10.1021/acscatal.0c02222
ACS Catal. 2020, 10, 8590–8596

from the crystallization solution (one ASU only). No metal coordination sites were present in our UDP binary complex, consistent with the metal-independent nature of MGAT5 activity.

The extensive structural effects of UDP binding upon MGAT5 prompted us to investigate possible interactions between the enzyme donor and acceptor subsites. Attempts to generate a stable ternary substrate complex analogue using UDP-2FGlc (a nonhydrolyzable UDP-GlcNAc mimic) resulted in binding modes considered to be catalytically implausible (Figure S6). However, a ternary MGAT5+M592+UDP complex could be readily obtained by soaking MGAT5 crystals with both molecules (Figure 4a). UDP interactions to MGAT5 in this ternary complex were essentially identical to its binary complex and also induced Lys279−Gly293 loop ordering. In contrast, M592 was substantially displaced from its binary complex position by the now structured Lys279−Gly293 loop (Figure 4b; Figure S7a), enabling a water mediated H-bonding network to form between UDP, Glu297, and the acceptor α-mannose. Crucially, this H-bonding network involves a direct interaction between Glu297 and the α-mannose O6, creating a catalytically poised active site in which acceptor nucleophile deprotonation is possible. Although few direct interactions were observed between M592 and the Lys279−Gly293 loop (a CH-π bond between Phe283 and the central M592 mannose; Figure S7b), it appears that Lys279−Gly293 loop formation in itself sterically constrains the MGAT5 acceptor subsite, ensuring that acceptor glycans can only bind in catalytically productive configurations. Our data thus suggest a sequential bi-bi MGAT5 reaction profile,[23,24] in which UDP-GlcNAc binding likely precedes Lys279−Gly293 loop ordering and acceptor binding during Michaelis complex formation. We note that our studies with M592 do not preclude further interactions that may occur for *bona fide* protein N-glycan substrates, such as the contact between the chitobiose core and the MGAT5 protein surface previously postulated by Nagae.[19]

Given our new structural insights, notably the role of Lys279−Gly293 loop induced acceptor repositioning, we next sought to model the MGAT5 reaction using molecular dynamics (MD) and QM/MM methods, which can provide a comprehensive description of enzyme mechanism. We reconstructed a postulated MGAT5 Michaelis complex from the UDP+M592 ternary complex, via manual addition of a GlcNAc bound to the UDP β-phosphate, guided by the positions of existing active site waters (Figure S8). MD simulations[25] (120 ns) confirmed that this complex was stable, reaching a maximum Cα root-mean-square-displacement of ∼1.5 Å after 20 ns (Figure S9). M592 appeared relatively mobile in the acceptor subsite, adopting two main substrate poses, with the major pose corresponding to a state well-poised for nucleophilic attack (Figure S10).

QM/MM metadynamics simulations were initiated from a representative snapshot of the MD simulation in its major pose.[26,27] The QM region was described with density functional theory (DFT), using the Perdew−Burke−Ernzerhof (PBE) functional, whereas the MM region was described with the Amber force field (see Supporting Information). The reaction was driven from reactants to products using a single collective variable (CV), which combines the main bonds formed and cleaved during the reaction. The CV was defined as the difference of C1−O_{UDP} (the GlcNAc-phosphate bond) and C1−O6 (the GlcNAc bond to the acceptor α-mannose O6) distances. This chosen CV does not self-select any specific reaction pathway, and crucially, does not dictate whether Glu297 is part of the reaction pathway.

Analysis of the simulated reaction free energy profile provides an atomistic picture of the MGAT5 catalytic mechanism (Figure 5; Supporting Video). A pre-Michaelis complex (**MC′**) in the region of the reactants state is formed, in which Glu297 is not yet coordinated to M592. **MC′** is separated from the true Michaelis complex (**MC**) by a small energy barrier (∼2.5 kcal.mol^{-1}), corresponding to subtle repositioning movements that enable H-bonding between Glu297 and $O6_{Man}$−H, a prerequisite for proton transfer later in the reaction. The enzyme at **MC** is well-poised for catalysis, with the acceptor α-mannosyl O6 lying 3.36 Å from the GlcNAc anomeric carbon (C1), almost perfectly oriented for in-line nucleophilic attack ($O6_{Man}$···C1−O_{UDP} ≈ 170°) (Table 2).

Glycosyl transfer proceeds toward the transition state (**TS**) via elongation of the bond between the UDP and GlcNAc moieties (C1−O_{UDP}), with a concurrent approach of the α-mannosyl acceptor. At **TS**, GlcNAc lies tightly sandwiched between the α-mannosyl acceptor and UDP β-phosphate, and it exhibits clear oxocarbenium ion character, exemplified by a distorted $^4H_3$ ring conformation (vide infra), reduced C1−O5 bond length, and increased positive charge at C1 (Figure 5; Table 2). We also observed partially broken/formed C1−O_{UDP} and C1−$O6_{Man}$ bonds, respectively; an elongated $O6_{Man}$−H bond; and a shortened H-bonding distance between the acceptor O6 and the Glu297 sidechain ($O6_{Man}$−H···O_{Glu297}). The reaction resolves toward the product state (**P**) as the $O6_{Man}$−H proton transfers onto Glu297, confirming its role as catalytic base, while GlcNAc moves toward $O6_{Man}$, forming the new β-1,6 glycosidic bond. Our computed reaction free-energy profile exhibits a single transition state, indicative of a concerted mechanism, with a free energy barrier (15 kcal·mol^{-1}) consistent with that estimated from the experimental rate constant (∼17 kcal·mol^{-1}).

Conformational ring distortions are commonly employed by glycoside hydrolases (the enzymes that cleave glycosidic bonds) as a strategy to facilitate nucleophilic displacement.[28] However, despite some mechanistic similarities, ring distortions have to date remained unreported in inverting glycosyltransferases. Our QM/MM simulation revealed a distinct conformational itinerary for the GlcNAc ring during its transfer from donor to

Table 2. Relevant Parameters Involving the Donor and Acceptor at Each Characteristic Point along the Reaction Coordinate[a]

structural parameter	MC	TS	P
	Distance (Å)		
$C1_{GlcNAc}$-O_{UDP}	1.52 ± 0.06	2.45 ± 0.07	3.48 ± 0.06
$C1_{GlcNAc}$-$O6_{Man}$	3.36 ± 0.09	2.69 ± 0.08	1.50 ± 0.05
$O6_{Man}$-$H6_{Man}$	1.02 ± 0.04	1.04 ± 0.03	1.79 ± 0.25
$H6_{Man}$-O_{Glu297}	1.69 ± 0.16	1.65 ± 0.24	1.02 ± 0.03
$C1_{GlcNAc}$-$O5_{GlcNAc}$	1.38 ± 0.03	1.28 ± 0.03	1.39 ± 0.04
	Angle (deg)		
$O6_{Man}$···C1−O_{UDP}	169.42 ± 5.51	168.42 ± 6.27	171.65 ± 4.11
	Charge[b]		
$C1_{GlcNAc}$	+0.07 ± 0.01	+0.15 ± 0.01	+0.06 ± 0.01

[a]Subscript labels refer to the molecule to which the atom belongs to at **MC**. [b]Restrained electrostatic potential atomic partial charge (RESP), in electron units.

https://dx.doi.org/10.1021/acscatal.0c02222
ACS Catal. 2020, 10, 8590−8596

acceptor. At **MC**, GlcNAc maintains a ground state $^4C_1$ ring conformation, as its axially oriented UDP leaving group is already well-poised for attack. As the GlcNAc anomeric center proceeds in its migration from UDP to M592 and the C1−O_{UDP} bond breaks, the sugar ring changes to a distorted $[^4H_3]^{\ddagger}$ conformation at **TS**, characteristic of an oxocarbenium ion-like species. Finally, formation of the new glycosidic bond with M592 is accompanied by H-bonding between the GlcNAc N-acetyl moiety and the tightly abutting α-mannose O4 and UDP β-phosphate groups, which enforce a distorted $^{1,4}B$ ring conformation even after glycosyl transfer (**P**)—a situation reminiscent of the product distortion sometimes observed for inverting glycoside hydrolases.[29,30] Relaxation of GlcNAc back to a ground state $^4C_1$ conformation likely accompanies diffusion of the product glycan out of the MGAT5 active site.

Overall, we have expanded considerably upon existing structural knowledge of MGAT5, by providing the first molecular characterization of MGAT5 donor subsite interactions, which revealed large rearrangements of the Lys279−Gly293 loop that are fundamental to the catalytic cycle. QM/MM simulations based upon our structural data provide a detailed description of MGAT5 catalyzed transfer, confirming the essential assisting role of Glu297 in the reaction mechanism and capturing the conformational itinerary undertaken by GlcNAc throughout its migration from donor to acceptor. Given its prominent role in cancer progression, there remains intense interest in the development of novel inhibitors to control pathological MGAT5 overactivity. Our work provides a comprehensive molecular overview of MGAT5 catalysis that will guide such inhibitor development efforts. Notably, strategies based upon conformational mimicry have successfully delivered inhibitors against many classes of glycoside hydrolases.[31,32] We suggest that pharmacological targeting of the MGAT5 donor subsite, using inhibitors inspired by conformational analysis, may also prove to be effective for the development of compounds to control the activity of this glycosyltransferase.

■ ASSOCIATED CONTENT

Supporting Information

The Supporting Information is available free of charge at https://pubs.acs.org/doi/10.1021/acscatal.0c02222.

Michaelis−Menten kinetics graphs, MGAT5 ribbon and surface representations, root-mean-square deviations between different MGAT5 crystal forms, STARANISO[2] calculated plots of reciprocal lattice points, comparison of M592 complex with previously reported MGAT5 acceptor complex, UDP-2FGlc ternary complex, MGAT5 acceptor subsite surfaces, analysis of protein atom root mean square displacements during the MD simulation timecourse, distribution of Michaelis complex C1−O6 distances during the MD simulation, data collection and refinement statistics, PDB accession codes, cloning primers, methods, and supporting references (PDF)

Video of the MGAT5 catalytic mechanism (MP4)

■ AUTHOR INFORMATION

Corresponding Authors

Carme Rovira − *Departament de Química Inorgànica i Orgànica (Secció de Química Orgànica) and Institut de Química Teòrica i Computacional (IQTCUB), Universitat de Barcelona, 08028 Barcelona, Spain; Institució Catalana de Recerca i Estudis Avançats (ICREA), 08020 Barcelona, Spain;* orcid.org/0000-0003-1477-5010; Email: c.rovira@ub.edu

Gideon J. Davies − *Department of Chemistry, University of York, Heslington, York YO10 5DD, U.K.;* orcid.org/0000-0002-7343-776X; Email: gideon.davies@york.ac.uk

Liang Wu − *Department of Chemistry, University of York, Heslington, York YO10 5DD, U.K.;* orcid.org/0000-0003-0294-7065; Email: liang.wu@rfi.ac.uk

Authors

John F. Darby − *Department of Chemistry, University of York, Heslington, York YO10 5DD, U.K.;* orcid.org/0000-0003-2754-6348

Amelia K. Gilio − *Department of Chemistry, University of York, Heslington, York YO10 5DD, U.K.;* orcid.org/0000-0003-2834-035X

Beatriz Piniello − *Departament de Química Inorgànica i Orgànica (Secció de Química Orgànica) and Institut de Química Teòrica i Computacional (IQTCUB), Universitat de Barcelona, 08028 Barcelona, Spain*

Christian Roth − *Department of Chemistry, University of York, Heslington, York YO10 5DD, U.K.*

Elena Blagova − *Department of Chemistry, University of York, Heslington, York YO10 5DD, U.K.*

Roderick E. Hubbard − *Department of Chemistry, University of York, Heslington, York YO10 5DD, U.K.;* orcid.org/0000-0002-8233-7461

Complete contact information is available at: https://pubs.acs.org/10.1021/acscatal.0c02222

Author Contributions

◆J.F.D., A.K.G., B.P.: These authors contributed equally.

Author Contributions

G.J.D., C.R., and L.W. conceived experiments. L.W. and Ch.R. cloned expression constructs. A.K.G. and Ch.R. produced proteins. J.F.D. and A.K.G. ran kinetics experiments. J.F.D., A.K.G., and E.B. carried out crystallization and ligand derivatizations. B.P. and C.R. carried out computational analyses. L.W. and C.R. wrote the manuscript with input from all authors.

Notes

The authors declare no competing financial interest.

■ ACKNOWLEDGMENTS

We thank Yorkshire Cancer Research, the European Research Council (ERC-2012-AdG-32294 "Glycopoise" to G.J.D.), the Biotechnology and Biological Sciences Research Council (BB/N008332/1 to R.E.H. and G.J.D.), the Spanish Ministry of Science and Innovation (AEI/FEDER, UE) (CTQ2017-85-496 to C.R.), the Spanish Structures of Excellence Maria de Maeztu (MDM-2017-0767 to C.R.), and the Agency for Management of University and Research Grants (AGAUR) (SGR2017-1189 to C.R.). B.P. thanks AGAUR for a predoctoral FI fellowship. G.J.D. thanks the Royal Society for the Ken Murray Research Professorship. We thank Diamond Light Source UK for access to beamline I03 and I04 (proposal mx-18598), the computer resources at the University of York High Performance Computing service (Viking and the Research Computing team), and the technical support provided by the Barcelona Supercomputing Center (BSC-CNS; Mare-Nostrum and CTE-Power supercomputers, project RES-BCV-2020-2-0009), which contributed to the results presented here. The authors thank

Professor Stephen G. Withers (University of British Columbia) for a kind gift of UDP-2FGlc.

REFERENCES

(1) Schwarz, F.; Aebi, M. Mechanisms and principles of N-linked protein glycosylation. *Curr. Opin. Struct. Biol.* **2011**, *21* (5), 576−582.
(2) Apweiler, R.; Hermjakob, H.; Sharon, N. On the frequency of protein glycosylation, as deduced from analysis of the SWISS-PROT database. *Biochim. Biophys. Acta, Gen. Subj.* **1999**, *1473* (1), 4−8.
(3) Ruggiano, A.; Foresti, O.; Carvalho, P. Quality control: ER-associated degradation: protein quality control and beyond. *J. Cell Biol.* **2014**, *204* (6), 869−879.
(4) Lee, H. S.; Qi, Y.; Im, W. Effects of N-glycosylation on protein conformation and dynamics: Protein Data Bank analysis and molecular dynamics simulation study. *Sci. Rep.* **2015**, *5*, No. 8926.
(5) Zhao, Y. Y.; Takahashi, M.; Gu, J. G.; Miyoshi, E.; Matsumoto, A.; Kitazume, S.; Taniguchi, N. Functional roles of N-glycans in cell signaling and cell adhesion in cancer. *Cancer Sci.* **2008**, *99* (7), 1304−1310.
(6) Moremen, K. W.; Tiemeyer, M.; Nairn, A. V. Vertebrate protein glycosylation: diversity, synthesis and function. *Nat. Rev. Mol. Cell Biol.* **2012**, *13* (7), 448−462.
(7) Pinho, S. S.; Reis, C. A. Glycosylation in cancer: mechanisms and clinical implications. *Nat. Rev. Cancer* **2015**, *15* (9), 540−555.
(8) Stanley, P. Golgi glycosylation. *Cold Spring Harbor Perspect. Biol.* **2011**, *3* (4), a005199.
(9) Nabi, I. R.; Shankar, J.; Dennis, J. W. The galectin lattice at a glance. *J. Cell Sci.* **2015**, *128* (13), 2213−2219.
(10) Lau, K. S.; Partridge, E. A.; Grigorian, A.; Silvescu, C. I.; Reinhold, V. N.; Demetriou, M.; Dennis, J. W. Complex N-glycan number and degree of branching cooperate to regulate cell proliferation and differentiation. *Cell* **2007**, *129* (1), 123−134.
(11) Partridge, E. A.; Le Roy, C.; Di Guglielmo, G. M.; Pawling, J.; Cheung, P.; Granovsky, M.; Nabi, I. R.; Wrana, J. L.; Dennis, J. W. Regulation of cytokine receptors by Golgi N-glycan processing and endocytosis. *Science* **2004**, *306* (5693), 120−124.
(12) Croci, D. O.; Cerliani, J. P.; Dalotto-Moreno, T.; Mendez-Huergo, S. P.; Mascanfroni, I. D.; Dergan-Dylon, S.; Toscano, M. A.; Caramelo, J. J.; Garcia-Vallejo, J. J.; Ouyang, J.; Mesri, E. A.; Junttila, M. R.; Bais, C.; Shipp, M. A.; Salatino, M.; Rabinovich, G. A. Glycosylation-dependent lectin-receptor interactions preserve angiogenesis in anti-VEGF refractory tumors. *Cell* **2014**, *156* (4), 744−758.
(13) Fukuta, K.; Abe, R.; Yokomatsu, T.; Kono, N.; Asanagi, M.; Omae, F.; Minowa, M. T.; Takeuchi, M.; Makino, T. Remodeling of sugar chain structures of human interferon-gamma. *Glycobiology* **2000**, *10* (4), 421−430.
(14) Granovsky, M.; Fata, J.; Pawling, J.; Muller, W. J.; Khokha, R.; Dennis, J. W. Suppression of tumor growth and metastasis in Mgat5-deficient mice. *Nat. Med.* **2000**, *6* (3), 306−312.
(15) Li, D.; Li, Y.; Wu, X.; Li, Q.; Yu, J.; Gen, J.; Zhang, X. L. Knockdown of Mgat5 inhibits breast cancer cell growth with activation of CD4+ T cells and macrophages. *J. Immunol.* **2008**, *180* (5), 3158−3165.
(16) Brockhausen, I.; Reck, F.; Kuhns, W.; Khan, S.; Matta, K. L.; Meinjohanns, E.; Paulsen, H.; Shah, R. N.; Baker, M. A.; Schachter, H. Substrate specificity and inhibition of UDP-GlcNAc:GlcNAc beta 1−2Man alpha 1−6R beta 1,6-N-acetylglucosaminyltransferase V using synthetic substrate analogues. *Glycoconjugate J.* **1995**, *12* (3), 371−379.
(17) Hanashima, S.; Inamori, K.; Manabe, S.; Taniguchi, N.; Ito, Y. Systematic synthesis of bisubstrate-type inhibitors of N-acetylglucosaminyltransferases. *Chem. - Eur. J.* **2006**, *12* (13), 3449−3462.
(18) Hassani, Z.; Saleh, A.; Turpault, S.; Khiati, S.; Morelle, W.; Vignon, J.; Hugnot, J. P.; Uro-Coste, E.; Legrand, P.; Delaforge, M.; Loiseau, S.; Clarion, L.; Lecouvey, M.; Volle, J. N.; Virieux, D.; Pirat, J. L.; Duffau, H.; Bakalara, N. Phostine PST3.1a Targets MGAT5 and Inhibits Glioblastoma-Initiating Cell Invasiveness and Proliferation. *Mol. Cancer Res.* **2017**, *15* (10), 1376−1387.
(19) Nagae, M.; Kizuka, Y.; Mihara, E.; Kitago, Y.; Hanashima, S.; Ito, Y.; Takagi, J.; Taniguchi, N.; Yamaguchi, Y. Structure and mechanism of cancer-associated N-acetylglucosaminyltransferase-V. *Nat. Commun.* **2018**, *9* (1), No. 3380.
(20) Korczak, B.; Le, T.; Elowe, S.; Datti, A.; Dennis, J. W. Minimal catalytic domain of N-acetylglucosaminyltransferase V. *Glycobiology* **2000**, *10* (6), 595−599.
(21) Tickle, I. J., Flensburg, C., Keller, P., Paciorek, W., Sharff, A., Vonrhein, C., Bricogne, G. *STARANISO* Global Phasing Ltd: Cambridge, UK, 2018. See the following: http://staraniso.globalphasing.org/cgi-bin/staraniso.cgi.
(22) Lairson, L. L.; Henrissat, B.; Davies, G. J.; Withers, S. G. Glycosyltransferases: structures, functions, and mechanisms. *Annu. Rev. Biochem.* **2008**, *77*, 521−555.
(23) Nishikawa, Y.; Pegg, W.; Paulsen, H.; Schachter, H. Control of glycoprotein synthesis. Purification and characterization of rabbit liver UDP-N-acetylglucosamine:alpha-3-D-mannoside beta-1,2-N-acetylglucosaminyltransferase I. *J. Biol. Chem.* **1988**, *263* (17), 8270−8281.
(24) Lira-Navarrete, E.; Iglesias-Fernandez, J.; Zandberg, W. F.; Companon, I.; Kong, Y.; Corzana, F.; Pinto, B. M.; Clausen, H.; Peregrina, J. M.; Vocadlo, D. J.; Rovira, C.; Hurtado-Guerrero, R. Substrate-guided front-face reaction revealed by combined structural snapshots and metadynamics for the polypeptide N-acetylgalactosaminyltransferase 2. *Angew. Chem., Int. Ed.* **2014**, *53* (31), 8206−8210.
(25) Case, D.A.; Ben Shalom, I. Y.; Brozell, S.R.; Cerutti, D.S.; Cheatham, T.E., III; Cruzeiro, V.W.D.; Darden, T.A.; Duke, R.E.; Ghoreishi, D.; Gilson, M.K.; Gohlke, H.; Goetz, A.W.; Greene, D.; Harris, R.; Homeyer, N.; Izadi, S.; Kovalenko, A.; Kurtzman, T.; Lee, T.S.; LeGrand, S.; Li, P.; Lin, C.; Liu, J.; Luchko, T.; Luo, R.; Mermelstein, D.J.; Merz, K.M.; Miao, Y.; Monard, G.; Nguyen, C.; Nguyen, H.; Omelyan, I.; Onufriev, A.; Pan, F.; Qi, R.; Roe, D.R.; Roitberg, A.; Sagui, C.; Schott-Verdugo, S.; Shen, J.; Simmerling, C.L.; Smith, J.; Salomon-Ferrer, R.; Swails, J.; Walker, R.C.; Wang, J.; Wei, H.; Wolf, R.M.; Wu, X.; Xiao, L.; York, D.M.; Kollman, P.A. *AMBER 2018*; University of California, San Francisco, 2018.
(26) Laio, A.; Parrinello, M. Escaping free-energy minima. *Proc. Natl. Acad. Sci. U. S. A.* **2002**, *99* (20), 12562−12566.
(27) Valsson, O.; Tiwary, P.; Parrinello, M. Enhancing Important Fluctuations: Rare Events and Metadynamics from a Conceptual Viewpoint. *Annu. Rev. Phys. Chem.* **2016**, *67*, 159−184.
(28) Ardèvol, A.; Rovira, C. Reaction Mechanisms in Carbohydrate-Active Enzymes: Glycoside Hydrolases and Glycosyltransferases. Insights from ab Initio Quantum Mechanics/Molecular Mechanics Dynamic Simulations. *J. Am. Chem. Soc.* **2015**, *137* (24), 7528−7547.
(29) Jin, Y.; Petricevic, M.; John, A.; Raich, L.; Jenkins, H.; Portela De Souza, L.; Cuskin, F.; Gilbert, H. J.; Rovira, C.; Goddard-Borger, E. D.; Williams, S. J.; Davies, G. J. A beta-Mannanase with a Lysozyme-like Fold and a Novel Molecular Catalytic Mechanism. *ACS Cent. Sci.* **2016**, *2* (12), 896−903.
(30) Petersen, L.; Ardevol, A.; Rovira, C.; Reilly, P. J. Mechanism of cellulose hydrolysis by inverting GH8 endoglucanases: a QM/MM metadynamics study. *J. Phys. Chem. B* **2009**, *113* (20), 7331−7339.
(31) Wu, L.; Armstrong, Z.; Schroder, S. P.; de Boer, C.; Artola, M.; Aerts, J. M.; Overkleeft, H. S.; Davies, G. J. An overview of activity-based probes for glycosidases. *Curr. Opin. Chem. Biol.* **2019**, *53*, 25−36.
(32) Speciale, G.; Thompson, A. J.; Davies, G. J.; Williams, S. J. Dissecting conformational contributions to glycosidase catalysis and inhibition. *Curr. Opin. Struct. Biol.* **2014**, *28*, 1−13.

https://dx.doi.org/10.1021/acscatal.0c02222
ACS Catal. 2020, 10, 8590−8596